Electronic Supporting Information (ESI)

Tailoring Two-dimensional Graphene Oxide Surface: Dual T_1 and T_2 MRI Contrast Agent Materials

Erwin Peng[*1], Fenghe Wang[1], Suhui Tan[1], Bingwen Zheng[2], Sam Fong Yau Li[2,3] and Jun Min Xue*[*1]*

[1]Department of Materials Science and Engineering, Faculty of Engineering, National University of Singapore (NUS), 7 Engineering Drive 1, Singapore 117574.

*Email: msexuejm@nus.edu.sg and mseer@nus.edu.sg

[2]Department of Chemistry, National University of Singapore, 3 Science Drive 3, Singapore 117543.

[3]NUS Environment Research Institute (NERI), Department of Chemistry, 3 Science Drive 3, Singapore 117573.

S1. Materials and Methods

Materials

Graphene oxide (GO) solution (at concentration of 5 mg/mL^{-1}) was purchased from Graphene Supermarket (New York) and pre-sonicated using probe-ultrasonicator (SONICS Vibracell VCX130) for 1 hour (pre-sonication time); the average hydrodynamic size for the pre-sonicated (1 hour) GO sheets in water was 258.0 ± 4.5 nm. For the hydrophobic nanoparticles synthesis, iron (III) acetylacetonate ($Fe(acac)_3$; 97%), manganese (II) acetylacetonate ($Mn(acac)_2$), manganese (II) acetate tetrahydrate ($Mn(CH_3COO)_2.4H_2O$), oleic acid (≥99%), benzyl ether (99%) and 1-octadecene (90%) were obtained from Sigma-Aldrich, Singapore. Chloroform ($CHCl_3$) and tetrahydrofuran (THF) solvents were obtained from Fisher Scientific. Cell Counting Kit-8 was also purchased from Sigma Aldrich, Singapore and stored at -20^{o}C.

Methods

Synthesis of Hydrophobic Mn-doped Fe_3O_4 Nanoparticles (T_2-NPs)

Typically, to obtain 10 nm hydrophobic manganese-doped (Mn-doped) Fe_3O_4 nanoparticles, 4 mmol of $Mn(acac)_2$, 8 mmol of $Fe(acac)_3$, 28 mmol of oleic acid and 35 mL of benzyl ether were charged into a 100 mL three-necks round bottom flask.[1] The flask was purged with N_2 gas for 30 minutes prior to the heating-up process in order to create inert environment. The mixture was then magnetically stirred and heated to 165^{o}C under N_2 gas flow protection, followed by a subsequent isothermal reaction for 30 minutes. Afterwards, the reaction temperature was further raised to reflux (~280^{o}C) and held isothermally for another 30 minutes. The resulting black-color solution was then allowed to cool down naturally. MnO nanoparticles was extracted from the resultant black-color solution mixture, collected and washed with the mixture of hexane/iso-propanol through repeated centrifugation and re-dispersion (10000 rpm; 10 mins; 20^{o}C). After the repeated purification, the resultant Mn-doped Fe_3O_4 nanoparticles were re-dispersed onto chloroform (at 50 mg.mL^{-1} concentration) and transferred to a glass vial for storage (at room temperature).

Synthesis of Hydrophobic MnO Nanoparticles (T_1-NPs)

Typically, to obtain 6nm hydrophobic MnO nanoparticles, 8 mmol of manganese (II) acetate tetrahydrate ($Mn(CH_3COO)_2.4H_2O$), 16 mmol of oleic acid and 30 mL of 1-octadecene were charged into a 100 mL three-necks round bottom flask. The flask was purged with N_2 gas for 30 minutes prior to the heating-up process in order to create inert environment. The mixture was then magnetically stirred and heated to 120^{o}C under N_2 gas flow protection, followed by a subsequent isothermal reaction for 1 hour. Afterwards, the reaction temperature was further raised to reflux (~320^{o}C) and held isothermally for another hour. The resulting black-color solution was then allowed to cool down naturally. MnO nanoparticles was extracted from the resultant black-color solution mixture, collected and washed with the mixture of hexane/acetone through repeated centrifugation and re-dispersion (15000 rpm; 10 mins; 5^{o}C). After the repeated purification, the resultant MnO nanoparticles were re-dispersed onto chloroform (at 50 mg.mL^{-1} concentration) and transferred to a glass vial for storage (at room temperature).

Synthesis of Water Soluble GO/T_2 or GO/T_1 Nanocomposites

The hydrophobic MNPs (either T_1-NPs or T_2-NPs) were decorated onto hydrophilic GO sheets through a simple process. Briefly, the hydrophobic MNPs in $CHCl_3$ were recovered by centrifugation and re-dispersed into THF (5 mg.mL^{-1}). Subsequently, the MNPs in THF were added to the GO solution (5 mg.mL^{-1}) in water, followed by further dilution with excess water. The mixture can then be homogenized by either using bath sonicator (10 minutes) or probe-ultrasonicator (SONICS Vibracell VCX130; synthesis sonication time; 2.5 - 3 minutes). The solution mixture of GO/MNPs in THF/water was then heated-up to 80^{o}C for 1 hour under magnetic stirring, in order to completely evaporate the volatile organic THF solvent. The resultant GO/MNPs, namely GO/T_2 (with T_2-NPs core) and GO/T_1 (with T_1-NPs core) nanocomposites were cooled down, centrifuged (3000 rpm; 10 mins) to remove unnecessary large aggregates and finally stored in glass vials.

Synthesis of Water Soluble GO/Dual Nanocomposites

To obtain GO/Dual nanocomposites, GO/MNPs-1 nanocomposites can be prepared beforehand using the aforementioned protocols. Subsequently, the resultant hydrophilic GO/MNPs-1 nanocomposites in water was used as the GO precursors and reacted with MNPs-2 in THF (5 mg.mL^{-1}). The mixture was then homogenized using probe-ultrasonicator (SONICS Vibra-cell

VCX130; 5 minutes). Similarly, the solution mixture of GO/MNPs in THF/water was then heated-up to 80^{o}C for 1 hour under magnetic stirring, in order to completely evaporate the volatile organic THF solvent. The resultant GO/MNPs-1/MNPs-2 (denoted as GO/Dual) were cooled down, centrifuged (3000 rpm; 10 mins) to remove unnecessary large aggregates and finally stored in glass vials. In this paper, MNPs-1 referred to Mn-doped Fe_3O_4 nanoparticles (T_2-NPs) while MNPs-2 referred to MnO nanoparticles (T_1-NPs).

Cell Cytotoxicity (CCK-8 Cytotoxicity Assay)

Breast cancer cells (MCF-7) were grown in in Dulbecco's Modified Eagle Medium (DMEM) culture growth medium, supplemented with 10% FBS and penicillin at 37^{o}C in 5% CO_2 humidified environment. Prior to the cytotoxicity assessment, the MCF-7 cells were detached from the culture flask (with Tripsin), washed with the aid of centrifugation and suspended into fresh culture growth medium mixture (DMEM/10%FBS/penicillin). The final stock solution was kept at 10.0 x 10^4 cells.mL^{-1} concentration. To the 96-wells plate (TPP), 0.1 mL of the MCF-7 cells stock solution was seeded to each well (10000 cells per well). The seeded cells were further allowed to grow for another 24 hours at 37^{o}C in 5% CO_2 humidified environment. Subsequently, 20 μL of various concentrations of either hydrophilic GO/T2, GO/T1 or GO/Dual nanocomposites (ranging from 7.81 μM [Mn+Fe] to 125.0 μM [Mn+Fe]) were injected into the 96-wells plate that has been seeded with the MCF-7 cells. The 96-wells plate was slightly agitated to ensure uniform dispersion and then further incubated at 37^{o}C for another 24 hours under similar conditions. Prior to the cell viability measurement, 10 μL of CCK-8 was added to each well and the 96-wells plate was incubated further for another 4 hours. The absorbance reading of the 96-wells plate was then taken spectrophotometrically using Synergy^{TM} H1 multi-mode microplate reader at 450 nm.

MR Relaxivity Measurement

The hydrophilic GO/T_2, GO/T_1 and GO/Dual magnetic nanocomposites dispersed in water, at different metal concentrations (ranging from 7.0 μM [Mn+Fe] to 196.0 μM [Mn+Fe]), were loaded into 1 mL disposable plastic syringe and sealed with paraffin film to prevent leakage. The MRI measurements of these samples were performed using Agilent 7 T MRI scanner. For the T_1 measurement, inversion-recovery fast spin-echo sequence with 8 inversion times (T_I; ranging

from 10 ms to 4 s) was employed. Meanwhile for the T_2 measurement, multi-slice multi-echo sequence was employed. [Others parameters: T_R = 6 s (for T_1) and 2 s (for T_2); matrix size = 128 x 128; field of view = 40 x 40 mm; slice thickness = 4 mm).

Materials Characterizations

The transmission electron microscopy (TEM) images and the high resolution TEM images of the hydrophobic MNPs and the resultant hydrophilic GO/MNPs nanocomposites were recorded by using JEOL-3010F TEM (300 kV). The TEM sample was prepared by dripping one drop of the sample solution onto TEM copper grid, followed by a simple air-drying process at ambient condition. From the TEM images, the average TEM size was calculated by averaging more than 200 MNPs sampling populations. The crystal structure of the hydrophobic MNPs and the resultant hydrophilic GO/MNPs nanocomposites were recorded on a powder diffractometer (Bruker D8 Advanced Diffractometer System) with Cu Kα source (1.5418 Å). The X-ray photoelectron spectroscopy (XPS) spectra of hydrophobic MNPs and hydrophilic GO/MNPs samples were taken by using an Axis Ultra DLD x-ray photoelectron spectrophotometer equipped with an Al Kα x-ray source (1486.69 eV). The energy step size of the XPS was 1 eV for the survey scans and 0.1 eV for the fine scans. The subtraction of the Shirley background composition analysis and the XPS peaks deconvolution were carried out by using Casa XPS (2.3.14 version). The XPS spectra were calibrated to the sp^2 hybridized carbon peak at 284.6 eV. The hydrodynamic sizes and size distributions of the resultant hydrophilic GO/MNPs nanocomposites were measured by using a Malvern Zetasizer Nano-ZS at room temperature. The magnetic properties of various hydrophobic and hydrophilic samples were measured by LakeShore Model 7407 Vibrating Sample Magnetometer (VSM) at 25^{o}C. The hydrophobic MNPs samples were air-dried for few days while the hydrophilic GO/MNPs nanocomposites samples were freeze-dried for few days, prior to the VSM measurement.

For the MR relaxivity measurement and the cell cytotoxicity study, the total metal (Mn and Fe) concentrations of hydrophilic GO/T_2, GO/T_1 and GO/Dual nanocomposites were analyzed by inductive coupled plasma optical emission spectroscopy (ICP-OES) analysis (Perkin-Elmer Dualview Optima 5300 DV ICP-OES system). Briefly, the ICP samples were prepared by firstly dissolving the hydrophilic nanocomposites in 37wt% HCl, followed by the removal of GO sheets through centrifugation (15000rpm, 10 minutes).

S2. Tuning the T_1-NPs and T_2-NPs Separation Distance

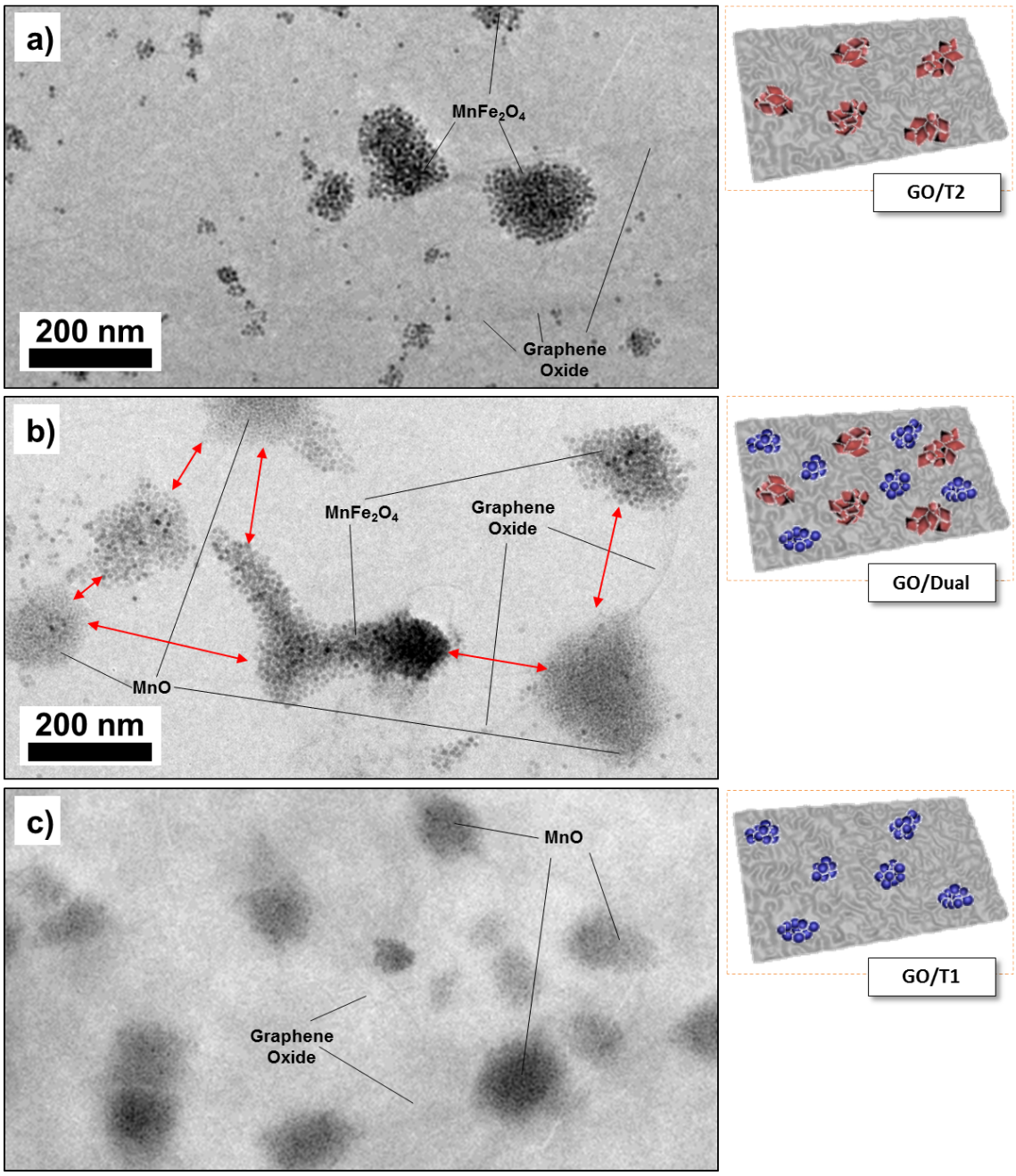

Fig. S1 (Left) Enlarge TEM images of hydrophilic (a) GO/T_2, (b) GO/Dual and (c) GO/T_1 nanocomposites dispersed in water. (Right) Schematic illustration of each respective nanocomposites.

From the TEM images of hydrophilic GO/Dual nanocomposites (**Fig. 2e,f** and **Fig. S1b**), the spacing distance between T_1-NPs and T_2-NPs clusters on GO sheets was more than 20 nm. Such separation distance was achieved due to the hydrophilic nanocomposites synthesis process that induced selective clustering of T_1-NPs and T_2-NPs (initially dispersed in THF) and deposition

into the hydrophobic segments of the GO sheets (dispersed in water) at different synthesis stages. In order to tune the separation distance between the T_1-NPs and T_2-NPs on GO sheets, a simply strategy by varying the hydrophobic nanoparticles to GO precursors mass ratio during the nanocomposites synthesis can be adopted accordingly. In the attempt to demonstrate this strategy, single-modality contrast agent nanocomposites comprising of T_1-NPs core was fabricated with different T_1-NPs (MnO nanoparticles) loading. Briefly, four different hydrophilic GO/T_1 nanocomposites with MnO:GO mass ratio of 0.667 (GO/T_1-A), 0.333 (GO/T_1-B), 0.167 (GO/T_1-C) and 0.083 (GO/T_1-D) were successfully fabricated. **Fig. S2** summarized the comprehensive materials characterization of various GO/T_1 nanocomposites synthesized with different T_1-NPs loading. From the TEM images analysis (see **Fig. S2a-d**) of several GO/T_1 nanocomposites, GO sheets became less saturated with T_1-NPs and the effective separation distance between the T_1-NPs clusters on GO sheets increased from few ten nanometers to few hundred nanometers with the decrease of the T_1-NPs loading.

At the same time, it was also observed from **Fig. S2e,f**, that the hydrodynamic size of the GO/T_1 nanocomposites increased accordingly with the increase in the hydrophobic nanoparticles proportion (*i.e.* increasing MnO:GO mass ratio). As the MnO:GO mass ratio was reduced from 0.667 to 0.333, 0.167 and 0.083, the hydrodynamic size decreased from 651.1 ± 9.9 nm to 361.1 ± 8.1 nm, 351.0 ± 3.4 nm and 297.4 ± 4.1 nm. The abrupt change in the hydrodynamic size at higher T_1-NPs loading can be ascribed to the need for greater hydrophobic region (basal plane) of GO sheets to stabilize more hydrophobic T_1-NPs nanoparticles. Consequently, more GO sheets were intra-connected through non-covalent hydrophobic-hydrophobic interactions, resulting in the increase in the hydrodynamic sizes.

Inevitably, the tuning of the distance between the hydrophobic nanoparticles clusters on GO sheets also influenced the MR relaxivities of the resultant hydrophilic magnetic nanocomposites. As summarized in the plot of $1/T_1$ and $1/T_2$ relaxation rates of various hydrophilic GO/T_1 nanocomposites in **Fig. S2g,h** and **Fig. S2i**, the decrease in T_1-NPs loading improved the overall MR relaxivities of the GO/T_1 nanocomposites. With the decrease in the T_1-NPs loading, the GO sheet was less saturated with hydrophobic T_1-NPs; thus the water diffusivity (water penetrability) along the GO sheets improved considerably. This further promoted the interaction between the diffused water and the hydrophobic T_1-NPs within GO sheets. As reflected from the T_1-weighted

images and T_2-weighted images (see **Fig. S2j**), concentration-dependent T_1-brightening and T_2-darkening effects respectively, for GO/T_1 nanocomposites of different loadings were observed.

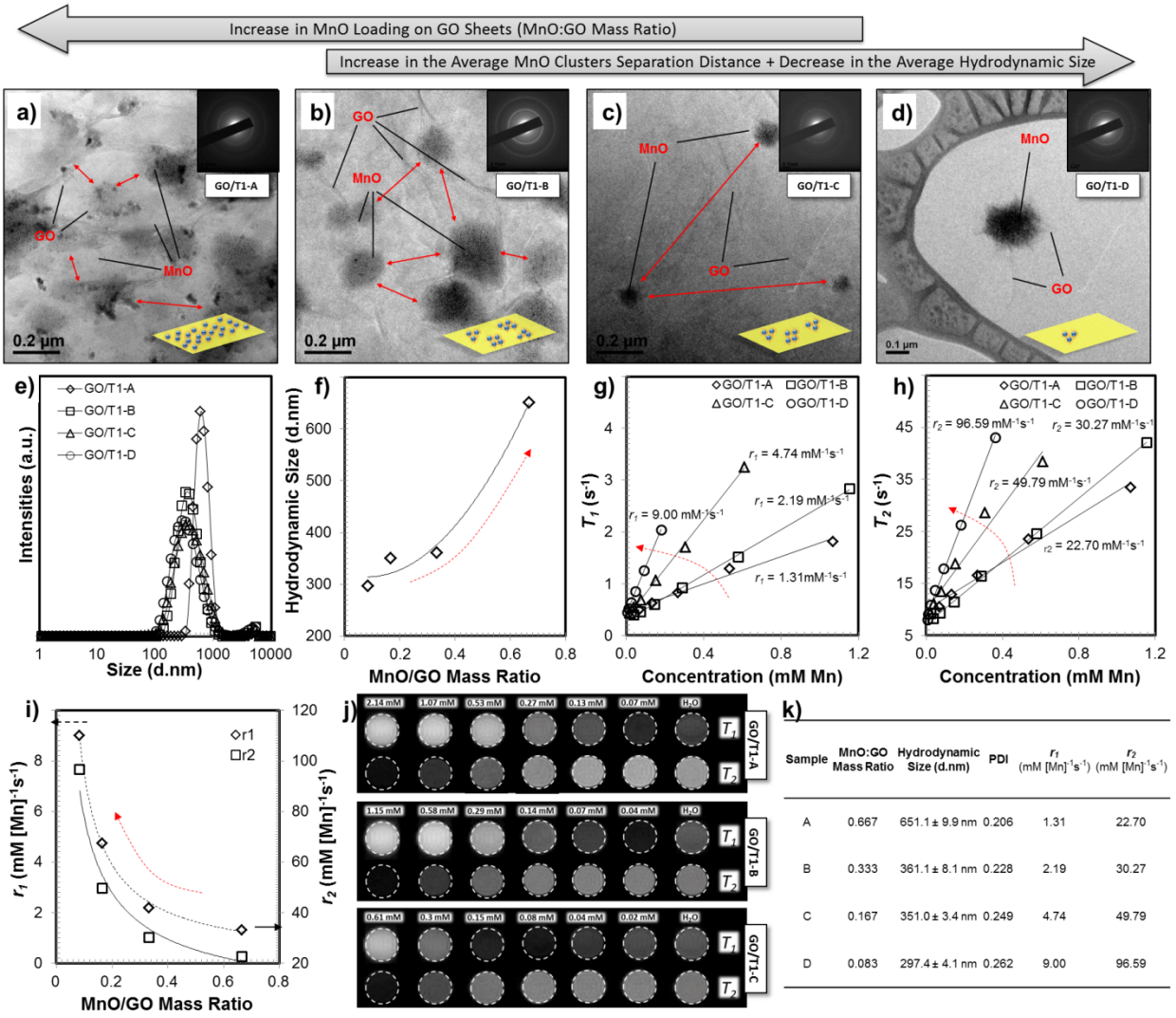

Sample	MnO:GO Mass Ratio	Hydrodynamic Size (d.nm)	PDI	r_1 (mM [Mn]$^{-1}$s^{-1})	r_2 (mM [Mn]$^{-1}$s^{-1})
A	0.667	651.1 ± 9.9 nm	0.206	1.31	22.70
B	0.333	361.1 ± 8.1 nm	0.228	2.19	30.27
C	0.167	351.0 ± 3.4 nm	0.249	4.74	49.79
D	0.083	297.4 ± 4.1 nm	0.262	9.00	96.59

Fig. S2 TEM images of GO/T_1 nanocomposites fabricated with different MnO:GO mass ratio (synthesis sonication time of 5 minutes): (a) MnO:GO = 0.667 (GO/T_1-A), (b) MnO:GO = 0.333 (GO/T_1-B), (c) MnO:GO = 0.167 (GO/T_1-C) and (d) MnO:GO = 0.083 (GO/T_1-D). (e) Hydrodynamic size distributions of various hydrophilic GO/T_1 samples in water (at 25°C). (f) Plot of average hydrodynamic sizes against the MnO:GO mass ratio. Plot of (g) 1/T_1 and (h) 1/T_2 relaxation rates of hydrophilic GO/T_1 nanocomposites with different MnO loadings. (i) Plot MR relaxivities of various hydrophilic GO/T_1 nanocomposites against the MnO:GO mass ratio. (j) Concentration-dependent T_1- and T_2-weighted images of hydrophilic GO/T_1 nanocomposites with different MnO loadings. (k) Tabulated data for various GO/T_1 nanocomposites.

Through the simple demonstration using only hydrophobic T_1-NPs, the aforementioned strategy to tune the separation distance between the hydrophobic nanoparticles clusters can be readily extended to the synthesis of GO/Dual nanocomposites.

S3. Tuning the Nanocomposites Average Hydrodynamic Size

Overall, there were three different possible strategies attempted to obtained hydrophilic nanocomposites with smaller hydrodynamic sizes: (i) Tuning the loading of the hydrophobic nanoparticles on GO sheets (by varying the total nanoparticles to GO mass ratio), (ii) Further sonication attempt during the nanocomposites synthesis process to further break-up the pre-sonicated GO sheets and lastly (iii) The addition of small hydrophilic molecules (*e.g.* mPEG-NH_2) during the hydrophilic nanocomposites synthesis process to prevent the re-stacking of the GO sheets.

(i) *Loading Tuning Attempt*

As highlighted in **Fig. S2** previously, tuning the loading of hydrophobic nanoparticles to GO sheets mass ratio influenced the resultant hydrophilic magnetic nanocomposites average hydrodynamic size. The hydrodynamic size of the hydrophilic magnetic nanocomposites decreased with the decrease in the nanoparticles loading. In general, this method was also restricted by the original size of the GO sheets precursor. For instance, the smallest nanocomposites GO/T_1-D (297.4 ± 4.1 nm) reported in **Fig. S2d** was slightly larger than the GO precursors used for the synthesis (258 ± 4.5 nm). Although it is possible to tune the nanocomposites hydrodynamic size by varying the the nanocomposites loading, such method may be ineffective for MRI application as the nanocomposites loading were typically correlated closely to its MR relaxivities.

(ii) *Further Sonication Attempt*

Alternatively, additional probe-sonication process can be carried-out to break-up the GO sheets precursors (or the resultant hydrophilic magnetic nanocomposites) into much smaller pieces. This method has been previously demonstrated to break-up nanoparticles/oleylamine-modified GO sheets nanocomposites.[2] **Fig. S3** summarized the attempts to reduce the size of the GO sheets (*i.e.* pre-sonication step) and the nanocomposites hydrodynamic size (*i.e.* synthesis sonication step). From the plot of GO hydrodynamic size against the probe-sonication time in **Fig. S3a**, the as-purchased GO sheets hydrodynamic size was 763.0 ± 11.5 nm. However, after 1 hour, 2 hours and 4 hours of probe sonication (by using Vibracell VCX130), the GO sheets

hydrodynamic size decreased to 258.0 ± 4.5 nm, 248.5 ± 10.6 nm and 243.7 ± 22.4 nm respectively.

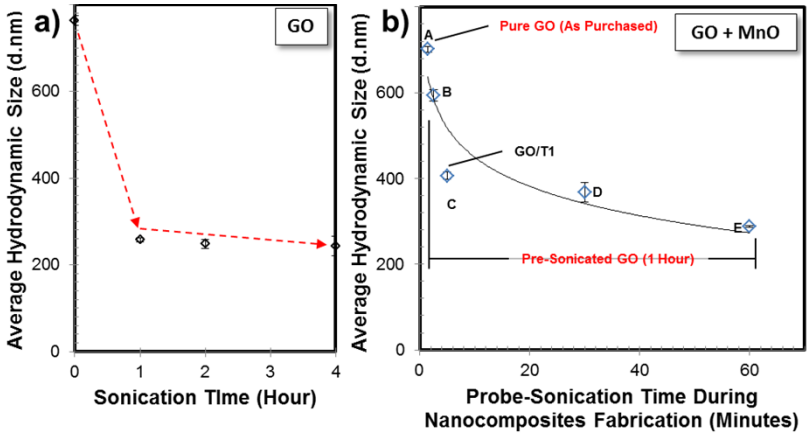

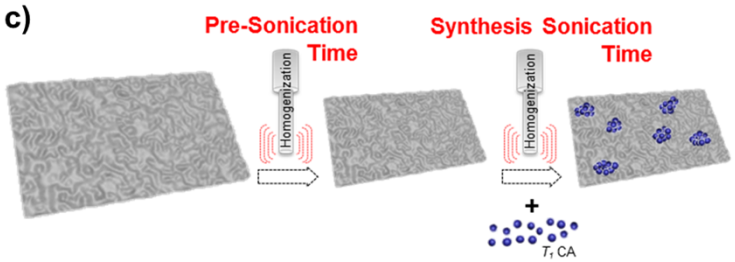

Sample	GO Pre-Sonication Time	GO/T1 Nanocomposites Synthesis Sonication Time	Hydrodynamic Size (d.nm)
A	0 Hour	1.5 Minutes	701.2 ± 6.9 nm
B	1 Hour	2.5 Minutes	593.3 ± 13.1 nm
C	1 Hour	5 Minutes	406.6 ± 8.2 nm
D	1 Hour	30 Minutes	367.9 ± 22.5 nm
E	1 Hour	60 Minutes	287.3 ± 1.9 nm

Fig. S3 (a) Plot of GO sheets hydrodynamic size in water (at 25°C) at different sonication time. (b) Plot of GO/T_1 nanocomposites hydrodynamic size at different probe-sonication time during nanocomposites fabrication process. (c) Illustration of pre-sonication time and synthesis sonication time.

Without any pre-sonication treatment, the resultant GO/T_1 nanocomposites formed using the as-purchased GO precursor was 701.2 ± 6.9 nm in hydrodynamic size. This was comparable with the original as-purchased GO sheets precursor hydrodynamic size (763.0 ± 11.5 nm). Meanwhile, the GO sheets precursor employed to fabricate GO/T_2, GO/T_1 and GO/Dual nanocomposites (**Fig. 2**) was pre-sonicated for 1 hour prior to the synthesis of the GO/T_2, GO/T_1 and GO/Dual nanocomposites. The resultant GO/T_2, GO/T_1 and GO/Dual nanocomposites hydrodynamic sizes (452.9 ± 14.2 nm, 406.6 ± 8.2 nm and 275.4 ± 17.7 nm respectively; presented in **Fig. 2)** were larger than their original GO sheets precursors (258 ± 4.5 nm). This

was ascribed to the possible re-stacking of GO sheets during the hydrophobic nanoparticles stabilization. From **Fig. S3b** whereby the pre-sonication time was kept at 1 hour, it was clearly observed from GO/T_1 nanocomposites that extended probe-sonication time during the nanocomposites synthesis process helped to break-up the GO sheets further (from 406.6 ± 8.2 nm to 287.3 ± 1.9 nm). While extended sonication time helped to break-up GO sheets and resulted in more hydrophilic oxygen-containing functional group (edge region), the GO sheets required to maintain certain proportion of the hydrophobic (basal region) segment in order to host the hydrophobic nanoparticles. As such, it was challenging to break down the GO further due to the need for balance between the hydrophobic and hydrophilic regions.

(iii) *PEGylation Attempt*

Lastly, in order to prevent GO sheets re-stacking as well as to promote the formation of much smaller and compact hydrophilic magnetic nanocomposites, small biocompatible molecules such as polyethylene glycol (PEG) can be added during the synthesis. In order to demonstrate this, short chain hydrophilic amine-polyethylene glycol or mPEG-NH_2 (MW 2000 or MW 5000) was mixed with the pre-sonicated GO sheets (1 hour) precursors prior to the hydrophilic nanocomposites formation. By mixing mPEG-NH_2 with small GO sheets, mPEG-NH_2 can attach onto GO sheets through chemisorption process in which ionic bonding was created between the amine group from mPEG-NH_2 and the carboxylic acid (–COOH) functional group from GO sheets through the formation of $COO^-|NH_3^+$ bonding. [3-4] The incorporation of mPEG-NH_2 onto GO sheets was expected to alter the hydrophobic-hydrophilic balance of the GO sheets, increasing its hydrophilicity. This configuration allowed greater electrostatic repulsion between the GO sheets and therefore, in the presence of hydrophobic nanoparticles, the re-stacking of GO sheets to form larger nanocomposites can be potentially avoided.

At similar synthesis formulation with GO/T_2, GO/Dual and GO/T_1, various hydrophilic nanocomposites were fabricated with mPEG-NH_2/GO precursors, namely GO/T_2-PEG2000, GO/Dual-PEG2000, GO/T_1-PEG2000 and GO/T_1-PEG5000. **Fig. S4** summarized the attempts to reduce the nanocomposites size by replacing GO precursors with mPEG-NH_2/GO precursors. The TEM images of GO/T_2-PEG2000 (**Fig. S4a,e**), GO/Dual-PEG2000 (**Fig. S4b,f**), and GO/T_1-PEG2000 (**Fig. S4c,g**) indicated a similar morphology to GO/T_2, GO/Dual and GO/T_1 (**Fig. 2c-h**) in which the hydrophobic nanoparticles were preferentially aggregated and decorated at the

hydrophobic segment of GO sheets basal plane due to hydrophobic-hydrophobic interaction. The TEM images of GO/T_1-PEG5000 (**Fig. S4d,h**), however, indicated that nanocomposites with different morphology than GO/T_1-PEG2000 and GO/T_1 has been successfully fabricated. Instead of two-dimensional nanostructures, the TEM images of GO/T_1-PEG5000 suggested the successful formation of three-dimensional nanostructures in which the mPEG-NH_2/GO precursors behaved similarly to the conventional amphiphilic polymers that wrapped around the hydrophobic nanoparticles clusters.[5-7] With the incorporation of the mPEG-NH_2 into the nanocomposites fabrication process, the hydrodynamic size of the resultant GO/T_2-PEG2000, GO/Dual-PEG2000, GO/T_1-PEG2000 nanocomposites were significantly reduced from its original GO/T_2, GO/Dual and GO/T_1 nanocomposites. From DLS measurement at 25^{o}C, the overall average hydrodynamic size of GO/T_2-PEG2000, GO/Dual-PEG2000, GO/T_1-PEG2000 and GO/T_1-PEG5000 nanocomposites were 164.8 ± 1.3 nm, 174.7 ± 1.9 nm, 202.2 ± 4.2 nm and 222.5 ± 4.2 nm. The significant decrease in the hydrodynamic size can be attributed to the successful GO sheets re-stacking inhibition.

The MR relaxivity measurements were also performed for GO/T_2-PEG2000, GO/Dual-PEG2000, GO/T_1-PEG2000 and GO/T_1-PEG5000 using 7T MRI scanner. From the plot of T_1 and T_2 relaxation rates against various metal concentration (see **Fig. S4j,k**), the r_1 values were 1.49 mM $[Mn+Fe]^{-1}s^{-1}$, 2.97 mM $[Mn+Fe]^{-1}s^{-1}$, 4.57 mM $[Mn]^{-1}s^{-1}$ and 3.68 mM $[Mn]^{-1}s^{-1}$ for GO/T_2-PEG2000, GO/Dual-PEG2000, GO/T_1-PEG2000 and GO/T_1-PEG5000 respectively. Meanwhile, the r_2 values were 54.27 mM $[Mn+Fe]^{-1}s^{-1}$, 93.51 mM $[Mn+Fe]^{-1}s^{-1}$, 42.59 mM $[Mn]^{-1}s^{-1}$ and 37.10 mM $[Mn]^{-1}s^{-1}$ for GO/T_2-PEG2000, GO/Dual-PEG2000, GO/T_1-PEG2000 and GO/T_1-PEG5000 respectively. From the summary (**Fig. S4l**), similar trend to **Fig. 3c** was observed for GO/T_2-PEG2000, GO/Dual-PEG2000 and GO/T_1-PEG2000 samples whereby the r_1 value increased with the T_1-NPs loading while the r_2 value was enhanced with the combinatorial loading of both T_1-NPs and T_2-NPs. Moreover, if the r_1 value of the GO/Dual-PEG2000 was expressed in terms of the contributing Mn ion concentration only, the r_1 value of the GO/Dual-PEG2000 was 6.25 mM $[Mn]^{-1}s^{-1}$, which was significantly comparable with the r_1 value of the GO/T_1-PEG2000. Based on this comparison, the simultaneous presence of both T_1 CA and T_2 CA materials within GO/Dual-PEG2000 nanocomposites did not annihilate the original individual MRI relaxometric properties. Similar to GO/Dual nanocomposites, this can be attributed to the

notable separation distance of more than 20 nm between T_1 CA and T_2 CA at GO sheet (**Fig. S4b,f**).

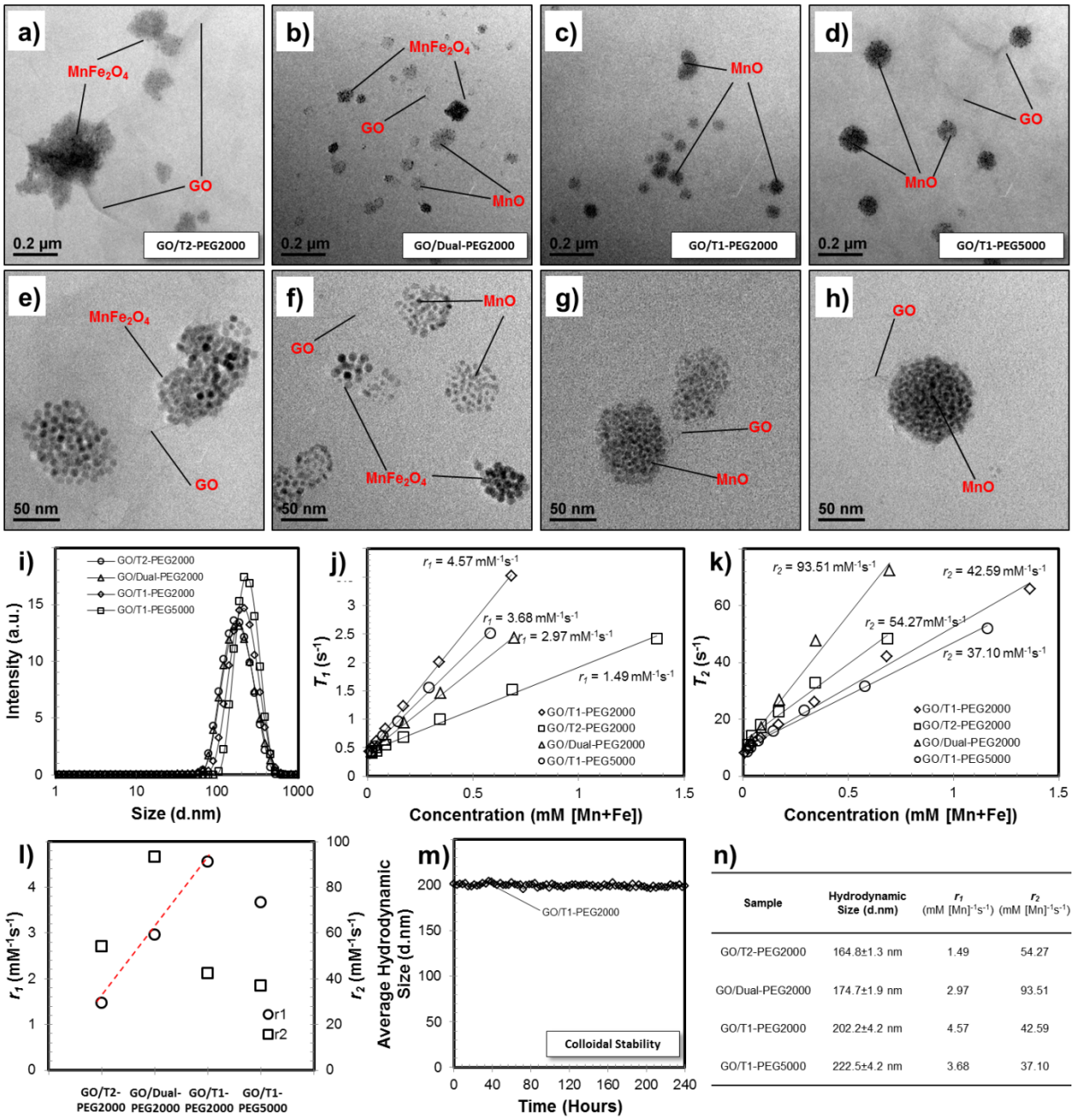

n)

Sample	Hydrodynamic Size (d.nm)	r_1 (mM [Mn]$^{-1}$s^{-1})	r_2 (mM [Mn]$^{-1}$s^{-1})
GO/T2-PEG2000	164.8±1.3 nm	1.49	54.27
GO/Dual-PEG2000	174.7±1.9 nm	2.97	93.51
GO/T1-PEG2000	202.2±4.2 nm	4.57	42.59
GO/T1-PEG5000	222.5±4.2 nm	3.68	37.10

Fig. S4 TEM images of various hydrophilic nanocomposites synthesized with the addition of mPEG-NH_2: (a,e) GO/T_2-PEG2000, (b,f) GO/Dual-PEG2000, (c,g) GO/T_1-PEG2000 and (d,h) GO/T_1-PEG5000. (i) Hydrodynamic size distributions of various hydrophilic nanocomposites samples in water (at 25°C). (j) $1/T_1$ and (k) $1/T_2$ relaxation rates of various hydrophilic nanocomposites. (l) MR relaxivities summary of various hydrophilic nanocomposites. (m) Colloidal stability of GO/T_1-PEG2000 in water at 25°C for 240 hours. (n) Tabulated data for various hydrophilic nanocomposites.

Based on the MR relaxivity results comparison, the overall relaxometric properties of hydrophilic nanocomposites formed using mPEG-NH_2/GO (GO/T_2-PEG2000, GO/Dual-PEG2000, GO/T_1-PEG2000) precursors were below than the relaxometric properties of hydrophilic nanocomposites formed using GO precursors only (GO/T_2, GO/Dual and GO/T_1). This can be ascribed to the presence of the mPEG-NH_2 on GO sheets that hindered the water permeation and diffusivity into the nanocomposites; thus lowering the effective relaxivity rates. Such effect of mPEG-NH_2 can also be clearly observed from the relaxometric properties comparison between GO/T_1-PEG2000 with GO/T_1-PEG5000 sample. With the presence of longer PEG chain, the r_1 value of GO/T_1-PEG5000 was approximately 19% lower than the r_1 value of GO/T_1-PEG2000. Lastly, the nanocomposites formed using mPEG-NH_2/GO precursors were also assessed for its colloidal stability. From **Fig. S4m**, GO/T_1-PEG2000 sample was stable in aqueous phase (25^{o}C) for more than 10 days without any significant hydrodynamic size changes.

Summary

Among the three aforementioned strategies, the nanocomposites PEGylation attempt was the most promising method to obtain smaller hydrophilic magnetic nanocomposites. Such PEGylation attempt, however, added more complexity to the synthesis system and caused slight decrease in the resultant nanocomposites relaxometric properties.

S4. Colloidal Stability of Nanocomposites

Despite the large reported average hydrodynamic size (more than 250 nm) of the GO/T_1, GO/T_2 and GO/Dual nanocomposites, the resultant hydrophilic magnetic nanocomposites can be stored for an extended period of time (more than 6 months) in water at ambient temperature/condition. The time-dependent colloidal stability of the GO/Dual nanocomposites was summarized in **Fig. S5** below. **Fig. S5a** showed the digital photograph of GO/Dual nanocomposites in aqueous solution after 6 months storage at ambient temperature. No significant precipitation was observed from the GO/Dual nanocomposites in aqueous solution. The absence of the observable aggregation implied that the loaded hydrophobic nanoparticles contrast agent were still intact with the GO sheets within the hydrophilic GO/Dual nanocomposites. From **Fig. S5b**, GO/Dual and one of the GO/T_1 nanocomposites were stable in aqueous phase for 48 hours.

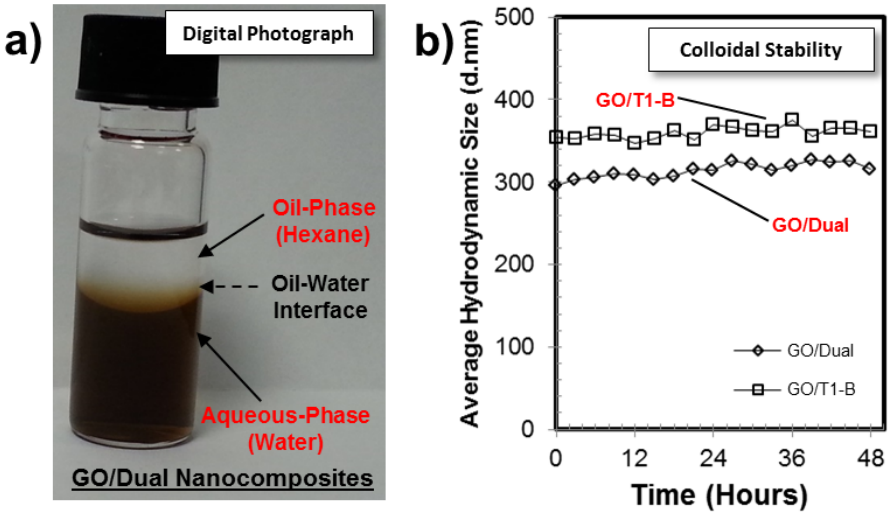

Fig. S5 (a) Digital photograph of GO/Dual nanocomposites in water after 6 months storage at room temperature. (b) Colloidal stability of GO/Dual and one of the GO/T_1 nanocomposites in water at 25^{o}C for 48 hours.

The digital photograph of GO/Dual nanocomposites also showed the hexane/water interface (with GO/Dual nanocomposites sample dispersed in water phase). If the nanoparticles fall off from the GO sheets, the hydrophobic nanoparticles were unlikely to be stable in aqueous phase with the presence of non-polar hexane phase. As there was no observable hydrophobic nanoparticles re-dissolution onto the oil-phase, it can be further concluded that the nanoparticles were indeed still intact with the GO sheets. On top of that, due to the hydrophobic nature of nanoparticles loaded onto the GO sheets, the synthesis mechanism to obtain GO/T_2, GO/T_1 and

GO/Dual nanocomposites relied heavily on the hydrophobic-hydrophobic interaction between the hydrophobic nanoparticles and the hydrophobic segments of the GO sheets (the basal plane; sp^2 carbon). As such, it is thermodynamically not favorable for the hydrophobic nanoparticles to detach from the GO sheets.

Reference

1. L. Li, Y. Yang, J. Ding and J. Xue, *Chemistry of Materials*, 2010, **22**, 3183.
2. E. Peng, E. S. G. Choo, P. Chandrasekharan, C.-T. Yang, J. Ding, K.-H. Chuang and J. M. Xue, *Small*, 2012, 8, 3620-3630.
3. D. W.-P. Pang, F.-W. Yuan, Y.-C. Chang, G.-A. Li and H.-Y. Tuan, *Nanoscale*, 2012, 4, 4562-4570.
4. W. Yu, H. Xie, X. Wang and X. Wang, *Nanoscale Res Lett*, 2011, 6, 47.
5. J. Yuan, E. Peng and J. M. Xue, *Journal of Materials Research*, 2014, 29, 1626-1634.
6. E. S. Guang Choo, X. Tang, Y. Sheng, B. Shuter and J. Xue, *Journal of Materials Chemistry*, 2011, 21, 2310-2319.
7. E. Peng, E. S. G. Choo, C. S. H. Tan, X. Tang, Y. Sheng and J. Xue, *Nanoscale*, 2013, 5, 5994-6005.